Insights into micro-structure and separation mechanism of benzimidazole-linked polymer membrane for H_2/CO_2 separation

Shan, Meixia; Zhang, Jingjing; Cong, Shenzhen; Zhang, Yatao; He, Xuezhong; Kapteijn, Freek; Liu, Xinlei

DOI
10.1016/j.seppur.2024.127732

Publication date
2024

Document Version
Final published version

Published in
Separation and Purification Technology

Separation and Purification Technology 349 (2024) 127732

Contents lists available at ScienceDirect

Separation and Purification Technology

journal homepage: www.elsevier.com/locate/seppur

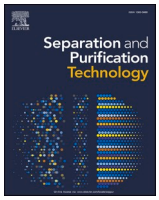

Insights into micro-structure and separation mechanism of benzimidazole-linked polymer membrane for H_2/CO_2 separation

Meixia Shan [a,f,*], Jingjing Zhang [a], Shenzhen Cong [c], Yatao Zhang [a,f], Xuezhong He [b,d], Freek Kapteijn [e], Xinlei Liu [c,*]

[a] School of Chemical Engineering, Zhengzhou University, Zhengzhou 450001, PR China
[b] Guangdong Provincial Key Laboratory of Materials and Technologies for Energy Conversion, Guangdong Technion - Israel Institute of Technology, Shantou, Guangdong 515063, PR China
[c] Chemical Engineering Research Center, School of Chemical Engineering and Technology, Tianjin Key Laboratory of Membrane Science and Desalination Technology, State Key Laboratory of Chemical Engineering, Tianjin University, Tianjin, 300350, China
[d] Department of Chemical Engineering, Guangdong Technion - Israel Institute of Technology, 241 Daxue Road, Shantou, Guangdong, 515063, PR China
[e] Chemical Engineering Department, Delft University of Technology, van der Maasweg, 9, 2629 HZ Delft, the Netherlands
[f] State Key Laboratory of Coking Coal Resources Green Exploitation, Zhengzhou University, Zhengzhou 450001, China

ARTICLE INFO

Keywords:
Benzimidazole-linked polymer
H_2/CO_2 separation
Interfacial polymerization

ABSTRACT

Separation of hydrogen from carbon dioxide for sustainable H_2 production and CO_2 capture still faces great challenges due to the smaller size of H_2 and higher condensability of CO_2. Herein, a high-performance benzimidazole-linked polymer (BILP) membrane for hydrogen separation was directly prepared on α-Al_2O_3 substrate through a facile interfacial polymerization approach at room temperature. The separation performance of the BILP membrane were regulated by controlling the reaction time and the microstructure was systematically characterized. Molecular simulations were performed to deep understand the separation mechanism in the BILP membrane. The best performance membrane displays an extraordinary mixed gas selectivity of 40 for H_2/CO_2 together with outstanding H_2 permeance of 250 gas permeation units (GPU) at 473 K, far exceeding the Robeson's upper bound. Besides, the membrane can withstand high temperature and pressure, and also shows good H_2/N_2 and H_2/CH_4 selectivity. The excellent separation performance, coupled with high temperature and pressure resistance and easy preparation, render BILP membranes great potential for economic H_2 purification, H_2 recovery, and natural gas treatment.

1. Introduction

Hydrogen, as a clean and reproducible energy source, holds great promise to solve energy shortages and energy-related environmental problems. However, great challenges exist to realize the hydrogen economy considering the high capital cost of hydrogen separation and purification processes, such as in steam methane reforming and hydrogen recovery from ammonia synthesis [1,2]. In this sense, membrane-based separation offers an effective and economic solution for H_2 separation and purification owing to the merits of greater energy efficiency, smaller units, easier operation and good compatibility with the environment [3,4]. Membrane materials that are highly selective for H_2 permeation over CO_2 at syngas processing conditions (423 K and above) are of particular industrial interest since they do not need to undergo syngas cooling before separation [5,6]. To achieve desired separation performance, manipulation of pore texture (e.g. *aperture* size, aperture size distribution and surface chemistry) is necessary [7–9]. One effective way to achieve superior H_2/CO_2 separation performance is to tune membrane systems with molecular-sieving pore structures into the desired size range since most of separations are based on a size-exclusion mechanism [10]. For example, Chuang *et al.* [11] incorporated three sulfocalixarenes molecules with different mean bottom opening size into poly[2,2′-(m-phenylene)-5,5′-bibenzimidazole] (PBI) to investigate the effect of cavity size on membrane separation performance towards H_2/CO_2 and found that the prepared membranes with smallest cavity sizes (~3.4 Å) showed strongest size-sieving effect towards H_2/CO_2. Yang *et al.* [12] designed an impressive size-sieving supramolecular array membrane using zero-dimensional 2-methylimidazole(mim) molecules

* Corresponding authors.
E-mail addresses: mxshan@zzu.edu.cn (M. Shan), xinlei_liu1@tju.edu.cn (X. Liu).

https://doi.org/10.1016/j.seppur.2024.127732
Received 22 February 2024; Received in revised form 9 April 2024; Accepted 27 April 2024
Available online 27 April 2024

through the precise design of the intermolecular spacing in the range between the size of H_2 and CO_2. The designed membrane displayed an unparalleled H_2/CO_2 separation coefficient of 3600, which is far higher than the values reported for a broad range of membranes. Xiao *et al.* [13] adopted a "prenucleation and slow growth" approach to prepare covalent organic framework (COF) membrane with highly oriented mesoporous channels and designed a gradient-channel segmentation methodology to control the nanochannel environments, thus leading to a remarkable H_2/CO_2 separation performance. However, such precise pore size generally does not exist in polymer membranes as gas transport mainly depends on the solution-diffusion mechanism. Gas molecules initially dissolve into the polymer and subsequently diffuse in the polymer network by breaking the interaction between polymer chains (π-π, hydrogen bond interaction, etc.), and are finally released from the membrane. In this case, promoting the diffusion of the small H_2 molecule to improve H_2/CO_2 selectivity is a valid approach to achieve excellent H_2/CO_2 separation performance. Polymer chain packing and chain stiffness play an important role in this H_2 diffusion process [14]. Various methods like polymer blending [15], cross-linking [16,17], inorganic particle incorporation [18], and chemical modification [19] have been proposed to change the chain packing behavior or chain stiffness to improve the gas permeability. For example, Wang *et al.* [14] introduced hydrazide into the polyimide backbone aiming at generating an abundant hydrogen-bond network to improve interchain interaction and further enhance the H_2/CO_2 size sieving selectivity.

Polybenzimidazoles (PBIs) [20–23], as the leading polymer for H_2/CO_2 membrane separation, exhibit excellent thermal stability and intrinsic H_2/CO_2 selectivity even at elevated temperatures. However, PBI shows low H_2 permeability because of the tightly polymer chain packing arising from π-π stacking and strong H-bond interactions. In addition to chain packing, chain length, molecular weight also influences the permeation of gases [24]. Benzimidazole linked polymers (BILPs) [25], composed of aromatic heterocyclic benzimidazole fused ring similar to PBIs, hold great promise for hydrogen separation owing to their high microporosity and robust organic backbone. Compared to linear PBIs with tightly packing chains, BILPs may achieve high gas permeability since they are composed by branched chains which will result in higher microporosity. While the preparation of defect-free BILP membrane in large-scale still faces great challenges since BILPs are generally insoluble in common solvents and most BILPs used in the membrane field is limited to blending with polymers to prepare mixed matrix membranes [26,27]. Interfacial polymerization (IP) method is facile to fabricate continuous and defect-free thin active layers in large area at the two phase interface, which has recently aroused attractive attention in preparing BILP membranes [28–34]. The possibility of room temperature IP for the fabrication of BILP-101x membrane for H_2/CO_2 separation was preliminarily identified in previous work [35]. The prepared membrane can withstand high pressure, showed high H_2/CO_2 selectivity (40 at 423 K) and exhibit excellent long-term hydro-thermal stability over 800 h under alternating dry and humid feed gas conditions, demonstrating the great potential of BILP membrane for H_2 separation under industrial relevant conditions. Despite its great potential, new strategies to improve the BILP-101x membrane gas permeance are still needed to increase the production of a membrane unit and cut costs of hydrogen separation.

Considering the high controllability of IP method, the chain packing behavior, chain length and the molecular weight of the formed membranes can be designed through adjusting IP synthesis parameters (monomer concentration, reaction solvent, reaction duration and temperature, catalysis concentration etc. [36–39]) to achieve better H_2/CO_2 separation performance. For example, Pinnau et al. [40] pointed out that increasing the trimesoyl chloride monomer concentration in aqueous solution or reaction temperature in organic phase can enhance the cross-linking degree of the formed membrane. The tightened polyamide membrane network greatly hindered the permeation of large molecules while has no significant effect on the transport of small gas molecules, thus improved the selectivity towards H_2. Through optimizing interfacial polymerization conditions, e. g. reaction time and monomer concentration, Livingston et al. [41] obtained an ultra-thin polyamide film with crumpled morphology demonstrating an ultrahigh acetonitrile permeance. From the above investigations, gas permeance and selectivity of IP-formed BILP membranes could be enhanced through controlling IP reaction conditions. Besides, the H_2/CO_2 separation mechanism of BILP-101x membrane also need to be clarified.

In this research, an ultra-selective and highly permeable BILP thin composite membrane was successfully prepared for H_2/CO_2 separation through controlling the IP reaction time. Single and mixed gas permeation tests were carried out across a pressure range up to 7 bara and temperatures up to 473 K. The microstructure of the prepared BILP-101x membrane were systematically investigated by a series of characterization techniques. Specially, positron annihilation lifetime spectroscopy (PALS) was performed to map the fraction free volume and pore size content of the BILP membranes prepared for different reaction time. In addition, molecular dynamic simulation was carried out to gain insight onto the H_2/CO_2 separation mechanism.

2. Experimental section

2.1. Synthesis of free-standing BILP-101x films

A 0.5 wt% TFB toluene solution was slowly poured on top of an aqueous BTA solution (1.5 wt%) in a big beaker at room temperature. A brown layer was appeared at the interface between water and toluene after several seconds. The interfacial polymerization reaction was left for 1, 2 or 3 h and then washed with toluene and deionized water. The prepared BILP-101x films were vacuum dried overnight at 373 K. A great many of films were collected following the same preparation procedure for further characterization.

2.2. Preparation of BILP-101x membranes

Alumina disks were first immersed in 1.5 wt% BTA aqueous solution in a small petri dish under 0.2 bar reduced absolute pressure for 20 min. The BTA containing substrates were dried using compressed air until no droplet can be observed on the surface and then immersed in a TFB toluene solution for 1, 2 and 3 h at room temperature, respectively. The prepared membrane was then taken out from the petri dish, left overnight in the fume hood and rinsed with toluene to remove residual monomers. Finally, the membrane was dried at room temperature and undergone performance test using a home-made permeation set-up [27].

2.3. Film and membrane characterization

Powder X-ray diffraction (PXRD) characterizations of BILP-101x films were done on a Bruker-D8 Advanced diffractometer. A Nicolet 8700 FT-IR (Thermo Scientic) was used to do the diffuse reflectance infrared Fourier transform (DRIFT) spectra. X-ray Photoelectron Spectroscopy (XPS) of BILP-101x film was carried out using a XPS PHI 5400 ESCA, mounted with a dual anode (Al/Mg). The morphology of BILP-101x films were obtained by a JEOL JSM-6010LA InTouchScope microscope. The surface and cross-sectional images of the supported BILP-101x membranes were acquired by a DualBeam Strata 235 microscope FEI) and an AURIGA Compact (Zeiss) microscope. N_2 (77 K) and CO_2 (273 K) adsorption isotherms of BILP-101x films were acquired by a Tristar II 3020 (Micromeritics). Thermogravimetric analysis (TGA) of BILP-101x films was carried out using a Mettler Toledo TGA/SDTA851e equipment. Positron annihilation lifetime spectroscopy measurements were performed to measure the fractional free volume (FFV) of BILP-101x films. Detailed characterization and calculation methods are provided in Supporting Information.

2.4. Gas permeation test

The prepared BILP-101x membrane was put into a home-made permeation setup for performance test. Single gas permeation tests were performed at 373 K and 1 bara pressure drop between the feed and permeate side. The mixed gas separation measurements were performed using an equimolar mixture of H_2 and CO_2, N_2 or CH_4 (50 mL·min^{-1} for each gas) as feed. Helium (4.9 mL·min^{-1}) was used in the permeate side. The absolute feed pressure was adjusted in a range of 1–7 bara using a back-pressure controller at the retentate side, and the permeate side was left at atmospheric pressure. The testing temperature in the permeation module was adjusted from 298 to 473 K through a convection oven. An on-line gas chromatograph (Interscience Compact GC) equipped with a packed Carboxen 1010 PLOT (30 m x 0.32 mm) column and TCD detector was used to periodically analyze the permeate stream. The permeance for the component A (P_a) can be calculated according to Equation 1:

$$P_a = \frac{N_a}{\Delta p_a \cdot A} = \frac{F_a}{\Delta p_a}$$

where F_a refers to the molar flux of component a (mol m^{-2} s^{-1}), N_a represents rate of compound a (mol/s) in the permeate, A represents the effective membrane area. Δp_a represents the partial pressure difference of compound a between the feed and permeate and is calculated based on Equation 2.

$$\Delta p_a = p_{feed} \times Y_{a,feed} - p_{perm} \times X_{a,perm}$$

where p_{feed} represents the absolute feed pressure and p_{perm} is the permeate pressure. $Y_{\text{a, feed}}$ and $X_{\text{a, perm}}$ refer to the mole ratios of compound a in the feed and permeate gas flows, respectively.

The SI unit for describing the gas permeance is mol·s^{-1}·m^{-2}·Pa^{-1}. However, polymeric membranes usually use GPU (Gas Permeation Unit) to assess the gas permeances, where 1 GPU = 3.35 x 10^{-10} mol·s^{-1}·m^{-2}·Pa^{-1}.

The mixed gas selectivity (α) was evaluated by the fraction the faster gas permeance (H_2 in this study), to the lower gas permeance (e.g. CO_2, N_2 and CH_4). For H_2/CO_2 separation, the α is written as equation 3.

$$\alpha_{H_2/CO_2} = \frac{P_{H_2}}{P_{CO_2}}$$

The ideal selectivity is similarly calculated as the ratio of the single component permeances.

3. Results and discussion

3.1. Characterization of BILP-101x films and membranes

The BILP-101x membrane was prepared onto an Al_2O_3 substrate through an in situ interfacial polymerization method (Fig. 1a).

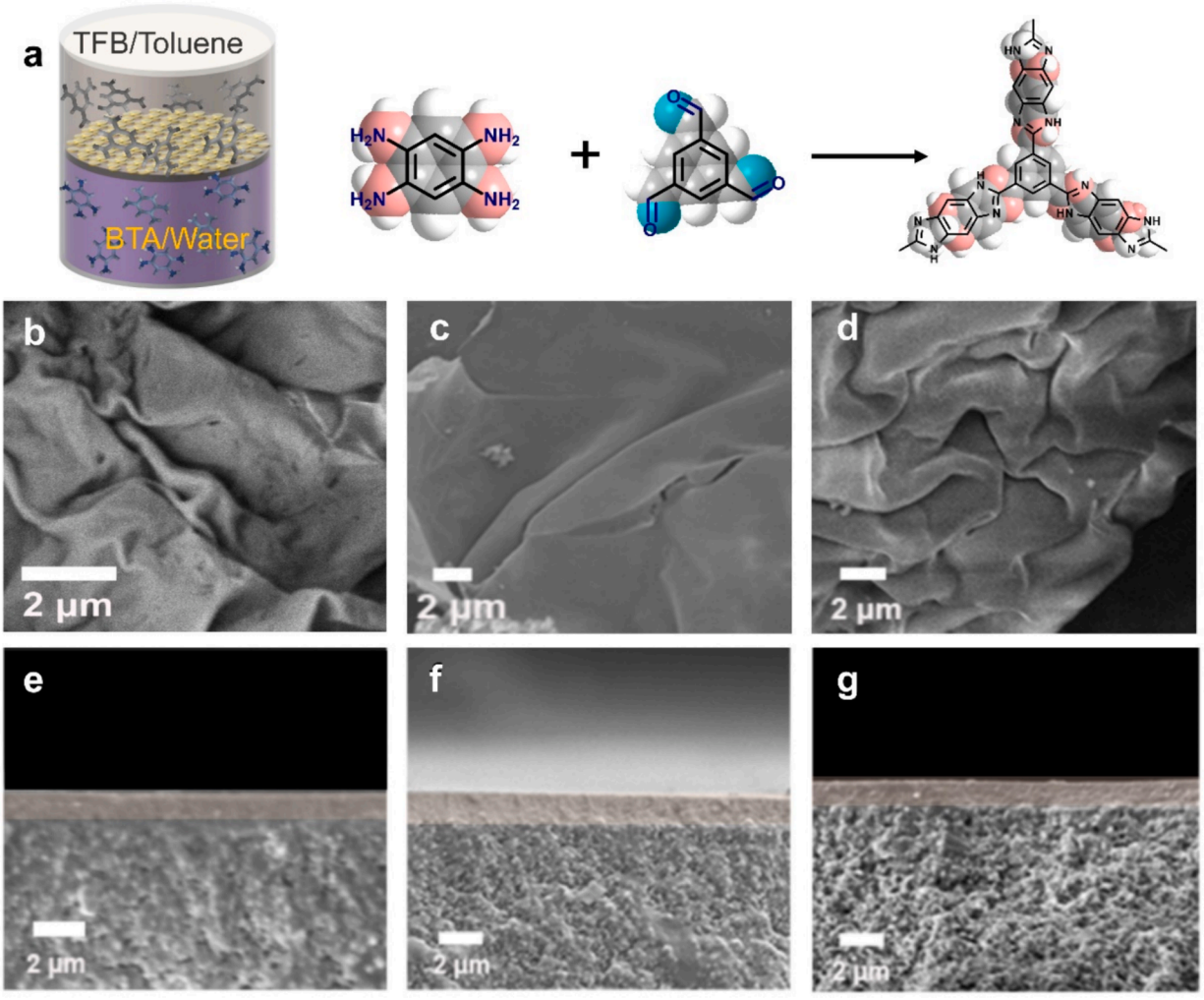

Fig. 1. (a) Illustration of the fabrication of BILP-101x membrane on Alumina substrate. (b-d) SEM images of free-standing films prepared with (b) 1 h (c) 2 h and (d) 3 h. Cross-sectional SEM images of (e)1h, (f) 2 h and (g) 3 h alumina substrate supported BILP-101x membrane.

Specifically, the Al_2O_3 substrate was first immersed into 1.5 wt% BTA-containing water solution for 20 mins under a reduced pressure of 0.2 bar. After sweeping out the excess water solution, the above BTA containing substrate was further contacted with 0.5 wt% TFB dissolved in toluene at the γ-Al_2O_3 side for different reaction duration (See details in Table 1). For convenient characterization of the microstructure of the membranes, free-standing BILP-101x films were also fabricated at the toluene-water interface under the same conditions. The reaction time shows a strong effect on the microstructure and separation performance of BILP-101x membranes. SEM images of the free-standing films exhibit a flexible, uniform, and continuous morphology (Fig. 1b-d). As can be calculated from cross-sectional SEM images, the thickness of the prepared membrane increases from 1.16 to 1.33 μm upon extending the reaction duration from 1 to 2 h and then stayed almost unchanged (the thickness of 3 h membrane is around 1.31 μm) (Fig. 1e-g), reflecting no further growth in thickness after 2 h.

TGA results demonstrate that all three membranes can withstand high temperature up to 523 K under Air atmosphere (Fig. S1). DRIFT spectroscopy of three samples (Fig. 2a) all revealed characteristic stretching bands at 1610 cm^{-1} and skeleton vibration at 1468, 1381 and 1242 cm^{-1}, confirming the successful formation of benzimidazole ring. Specially, the 2 h membrane film shows a relatively small peak area at 1701 cm^{-1} corresponding to the unreacted aldehyde monomers compared with the 1 and 3 h membrane films. This can be explained as follows: 1 h is not enough for finishing the reaction, as extending the reaction time to 2 h, more aldehyde monomers will diffuse to the interface and be consumed to form a defect-free film at the interface. As continue extending the reaction time, the aldehyde monomers diffuse to the interface while not react with BTA due to the barrier of defect-free film, leaving the aldehyde monomers on the membrane surface. The 2 h membrane films show the lowest CO_2 adsorption capacity (Fig. 2b), which can be attributed to the fewer $–NH_2$ groups left on the membrane, further supporting the more complete reaction of the 2 h membrane. Furthermore, as indicated by XRD spectra (Fig. 2c), the *d*-spacing of 2 h membrane chain is 3.5 Å, slightly larger than the other two membranes. The above observations are in agreement with the FFV results obtained by PALS (Table 2, the detailed information can be found in Supporting Information). As shown in Table 2, M2 membrane shows a slightly larger cavity size and fractional free volume compared to the M1 and M3 membranes, helpful for achieving higher gas permeance as discussed later.

Based on the above characterizations, we speculate that the chain packing of the 2 h membrane is different from the 1 h and 3 h membranes, possessing relatively more free volume and larger pore size. To further understand the effect of reaction duration on the microstructure of BILP-101x membranes, Fig. 3 illustrates the possible chain packing of BILP membranes to better understand the gas transport behavior through BILP-101x. Two kinds of possible gas transport in BILP-101x are envisaged. Fig. 3a, c shows the tightly packed pores formed by parallel chains, for which the strong π-π interaction and hydrogen bonding between polymer chains results in the compact chain packing [42]. In this case, gas molecules need to break these interactions (to form transient pores) to further travel in polymer membranes (Fig. 3f). Fig. 3b, d denotes the loosely packed pores (intrinsic pores) formed by entangled chains, where gas molecules can travel freely in the polymer membranes (Fig. 3f).

For the 1 h membrane, the reaction time was not enough for complete reaction thus leaving unreacted amine monomers in between the membrane chains. By prolonging the reaction time to 2 h, more aldehyde monomers will encounter the reactive functional groups to finish the reaction, forming polymer chains with fewer oligomers (Fig. 3f). When further prolonging the reaction time to 3 h, aldehyde monomers in the toluene solution may left among polymer chains. Overall, there are some oligomers or monomers left along 1 and 3 h membrane chains, forming hydrogen bonding with BILP-101x membranes which will increase the chain packing density and further block H_2 transportation to some extent. In case of the 2 h membrane, the reaction was relatively more complete with fewer monomers or oligomers left in the membrane, forming a loosely packed chain as indicated by PALS and XRD results, thus H_2 can be transported more freely in the membrane (Fig. 3f).

3.2. Gas separation performance

Each type of membranes (reaction duration 1, 2 and 3 h) were synthesized at least two times to make sure the separation results are reproducible. The detailed preparation conditions and separation performance of the prepared membranes are shown in Table 1. Fig. 4a shows the gas permeance and H_2/CO_2 selectivity of BILP-101x membranes at 423 K prepared for 1, 2 and 3 h, respectively. Prolonging the reaction time from 1 to 2 h increased both the H_2 permeance and H_2/CO_2 selectivity. As mentioned above, 1 h is not long enough for completely finishing the reaction and the unreacted amine monomers or small oligomers will increase the chain packing density through hydrogen bonding interaction thus will block H_2 transportation. Longer reaction duration, *i.e.* 2 h, will consume more unreacted monomers and leave more free volume for gas permeation [40], consistent with the FFV results calculated by PALS. However, upon further extending the reaction time to 3 h, the H_2 permeance and H_2/CO_2 selectivity start to decrease compared to the 2 h membrane. Overall, the 2 h BILP-101x membrane (M2) demonstrates the optimal separation performance towards H_2/CO_2 and is selected for further study.

Single gas permeation tests were performed at a constant feed pressure of 1 bara and 373 K using industrially important gas molecules including H_2, CO_2, N_2 and CH_4 (kinetic diameter of 2.89 Å, 3.3 Å, 3.64 Å and 3.8 Å, respectively). The membrane shows a sharp permeance cutoff between H_2 and the other three gases. The H_2/CO_2, H_2/N_2 and H_2/CH_4 selectivity are 21, 41, and 31, respectively, which are far exceeding the corresponding Knudsen diffusion selectivities (Fig. 4b). Considering the tightly chain packing of BILP-101x membranes, it is conceivably that the small H_2 molecules can diffuse through the transient pores while larger gases like CO_2, N_2, CH_4 are blocked, leading to the high selectivity. The higher CH_4 permeance than N_2 is because BILPs shows preferable adsorption on CH_4 over N_2 and similar observations have also been found in imidazole-linked polymer membranes [37].

The study of feed temperature and pressure was also applied to the other two duplicates of 2 h membranes, *i.e.*, M2-2 and M2-3. The same

Table 1
Summary of membrane preparation conditions and corresponding H_2/CO_2 separation performance at 423 K, 1 bara.

Membranes	Interfacial polymerization conditions			Membrane performance		
	Aqueous amine phase (wt.%)	Aldehyde in toluene phase (wt.%)	IP time (h)	H_2 Permeance (GPU)	CO_2 Permeance (GPU)	H_2/CO_2 selectivity
M1-1	1.5	0.5	1	101.8	3.91	26
M1-2	1.5	0.5	1	76.5	2.3	32.9
M2-1	1.5	0.5	2	135.4	2.88	47
M2-2	1.5	0.5	2	152	3.38	45
M2-3	1.5	0.5	2	122	2.93	41.4
M3-1	1.5	0.5	3	116.8	7.69	15.2
M3-2	1.5	0.5	3	72.3	2.34	22

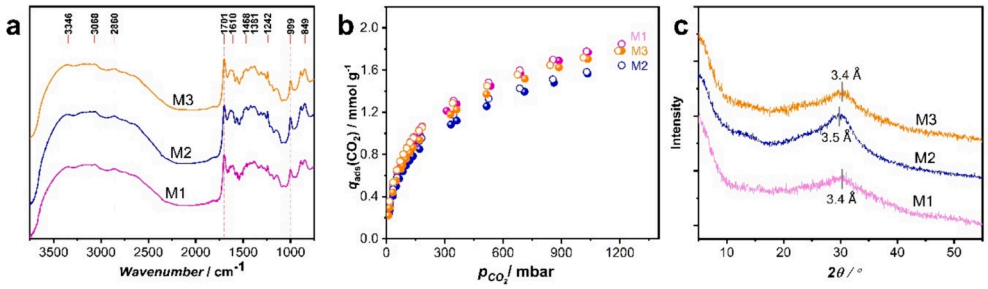

Fig. 2. (a) DRIFT spectra of BILP-101x films prepared for 1, 2 and 3 h reaction duration. (b) CO_2 adsorption (closed symbols) and desorption (opened circles) isotherms at 273 K and (c) PXRD patterns of BILP-101x films prepared for 1, 2 and 3 h reaction duration.

Table 2
The FFV% and free volume radius of three BILP-101x films calculated from PALS data. The detailed information of PALS data can be found in supporting Information.

Membrane	τ_3	I_3 (%)	R_3(Å)	FFV%
M1	2.395	1.594	3.19	0.391
M2	2.569	1.813	3.33	0.504
M3	2.372	1.558	3.17	0.371

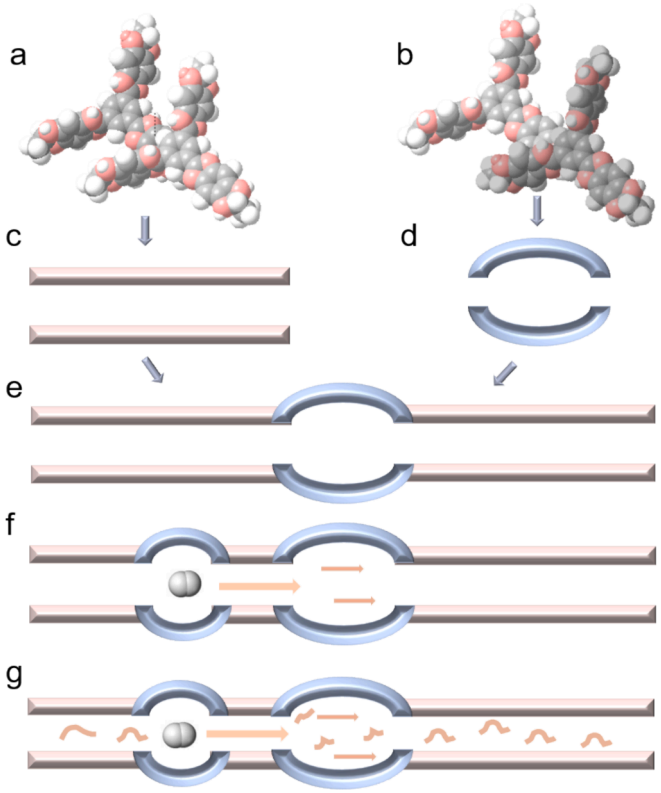

Fig. 3. Schematic diagram of pores formed by (a, c) the tightly-straight interchain packing and (b, d) the loosely-entangled chain packing. (e) Illustration of two kind of gas transport pores in BILP-101x membrane. Schematic diagrams of H_2 molecule transport in two kinds of pores without (f) or with monomers or oligomers (g) in BILP-101x membranes. (f) corresponds to IP duration of 2 h, and (g) corresponds to 1 or 3 h.

trend was observed as M2-1 (Fig. 5a). Both the H_2 and CO_2 gas permeance (in single and mixed gas test) increases with temperature, reflecting an activated transport. The temperature dependency of the permeation follows an Arrhenius equation for both the pure and mixed gas measurements (see details in Supporting Information, Fig. S3 and Table S1). BILP membrane shows higher CO_2 adsorption than H_2. Increase in temperature causes less adsorbed CO_2 which also causes a lower permeance. This effect is stronger than for H_2 due to its higher adsorption enthalpy. Activation energy for permeance is the sum of the intrinsic activation energy (expected to be higher for CO_2 due to its size) and the enthalpy of adsorption (negative value). Apparently, the net effect is that CO_2 has a lower activation energy for permeation. This is similar to that for zeolite membranes [43]. As shown in Table S1, the activation energy for H_2 is higher than CO_2 for both pure and mixed gas test, indicating that H_2 benefits more from temperature which leads to an enhancement in selectivity. Fig. 5b presents the pressure dependence of the pure and mixed gas permeance at 373 K. The gas permeances in the mixed gas measurement are slightly lower than that in the single gas test attributed to the competitive permeation.

The temperature and pressure stability were verified by a continuous, mixed gas permeation test. As presented in Fig. 6a, the 2 h membrane (*i.e.* M2-1) was first activated by increasing the temperature from 323 to 473 K. During this process, the H_2 permeance and H_2/CO_2 selectivity both increased dramatically. Specially, the membrane presented an outstanding H_2 permeance of 250 GPU and ultrahigh H_2/CO_2 selectivity of 40 at 473 K, which is of great interest for industrial pre-combustion CO_2 capture [44]. When the temperature was slowly lowered from 473 to 298 K, the H_2 permeance and H_2/CO_2 selectivity were even higher than during the heating-up procedure at the same temperature due to the activation. As the temperature further increased to 423 K at 141 h, the separation performances are comparable to the value tested at 67 h at the same conditions (1 bara, 423 K), pointing to good membrane durability. Afterwards, the membrane was tested more than 20 h at different pressures under 423 K and still exhibits excellent separation performance. Overall, the membrane can keep the good separation performance after high temperature and pressure treatment, indicating the potential application for long-term use.

To evaluate the BILP membrane material performance, the thickness of the membranes prepared under different reaction time were used for normalization. Fig.S2 presents the gas permeability and H_2/CO_2 selectivity of M1-M3 membranes, for which the 2 h membrane still exhibits the best performance. The H_2/CO_2 separation performance was further compared with the state-of-the-art PBI membranes and emerging porous organic framework membranes (PIMs and COFs) in a Robeson plot (Fig. 6b and Table S2) [45–48]. The supported BILP-101x membrane exhibits a superior separation performance with a H_2 permeability of 333 Barrer and H_2/CO_2 selectivity of 40 at 473 K (the thickness of the membrane was assumed as 1.33 μm based on cross-sectional SEM results), which far exceeds the Robeson upper bound line and are competitive with emerging micro-porous organic framework membranes such as PIMs and COFs. In addition to the application for H_2/CO_2 separation, the membrane also exhibits attractive separation performance towards H_2/N_2 and H_2/CH_4 (Fig. S4), demonstrating its great potential application in H_2 recovery and natural gas purification processes.

In order to deep understand the H_2/CO_2 separation mechanism in the

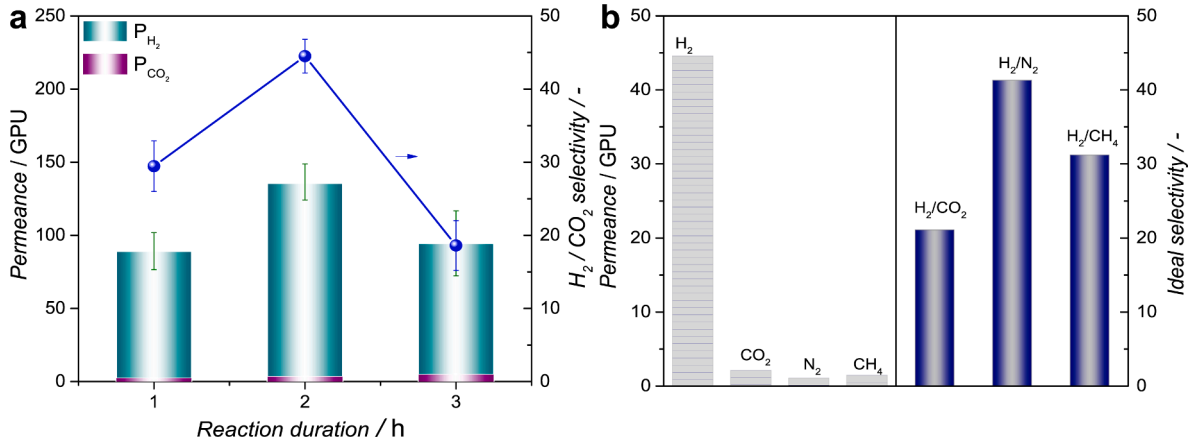

Fig. 4. (a) Effect of reaction duration (1, 2 and 3 h) on the mixed gas separation performance of BILP-101x membranes (M1, M2 and M3, respectively), tested at 423 K and 1 bara, and (b) Single gas permeation results of the BILP-101x membrane (M2-3) at 373 K and a pressure of 1 bara. Permeate side 1 bara He in both cases.

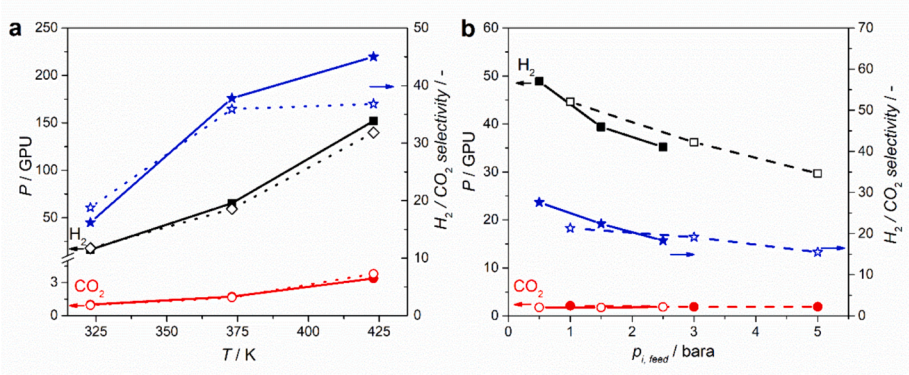

Fig. 5. (a) Influence of temperature on the H_2/CO_2 separation performance at 1 bara. (b) Influence of pressure on the H_2/CO_2 separation performance at 373 K. The data of Fig. 5a and b are obtained from membrane M2-2 and M2-3 respectively. Dashed and solid symbol correspond to single and equimolar mixed gas test, respectively.

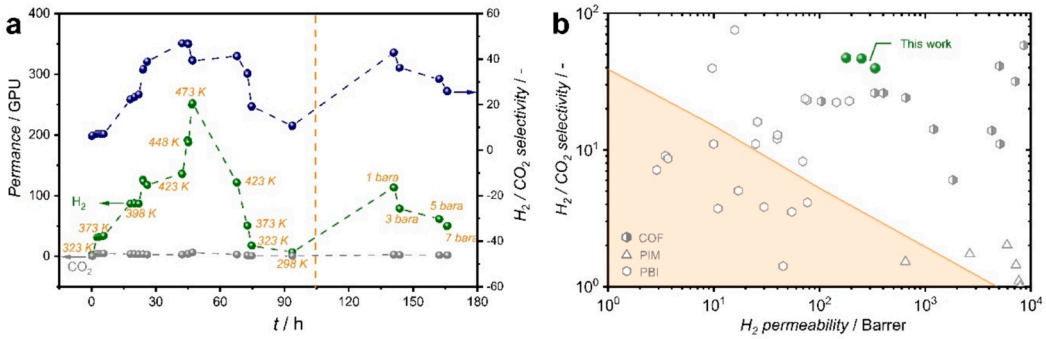

Fig. 6. (a) Performance stability of the M2-1 membrane under different temperatures (pressure kept at 1 bara) and pressures (temperature kept at 423 K). (b) Comparation of H_2/CO_2 separation performance with other polymer membranes in a Robeson plot. The yellow line is 2008 Robeson bound line [49]. See detailed data points in Table S2.

BILP-101x membrane, H_2 and CO_2 permeation behavior in the BILP-101x membrane were investigated using molecular dynamic simulations. Details of the simulation can be found in Supplementary Information. As shown in Fig. 7a and c, the initial configuration contains 500 H_2 and 500 CO_2 molecules in vacuum and 18 polymer chains of BILP-101x as the membrane module. After 200 ns simulation under NVT ensemble at 423 K, both H_2 and CO_2 gas molecules in the vacuum diffused into the polymer matrix (see end configurations in Fig. 7b and d) and the diffusion coefficients of H_2 calculated from the mean-square displacement are higher than that of CO_2 (Fig. 7e). This is reasonable considering that hydrogen has a smaller molecular size than carbon dioxide and moves easier from site to site in BILP-101x with narrow-pore size. While the amount of adsorbed CO_2 molecules is higher than H_2 (Fig. 7f), in line with previous research findings BILP shows strong interaction with CO_2 [50]. In this case, the adsorbed CO_2 will restrict the mobility of other CO_2 molecules (rather than H_2) due to the large cohesive energy of CO_2 than H_2. Thus, the permeation of H_2 is much faster than CO_2, resulting in the high selectivity.

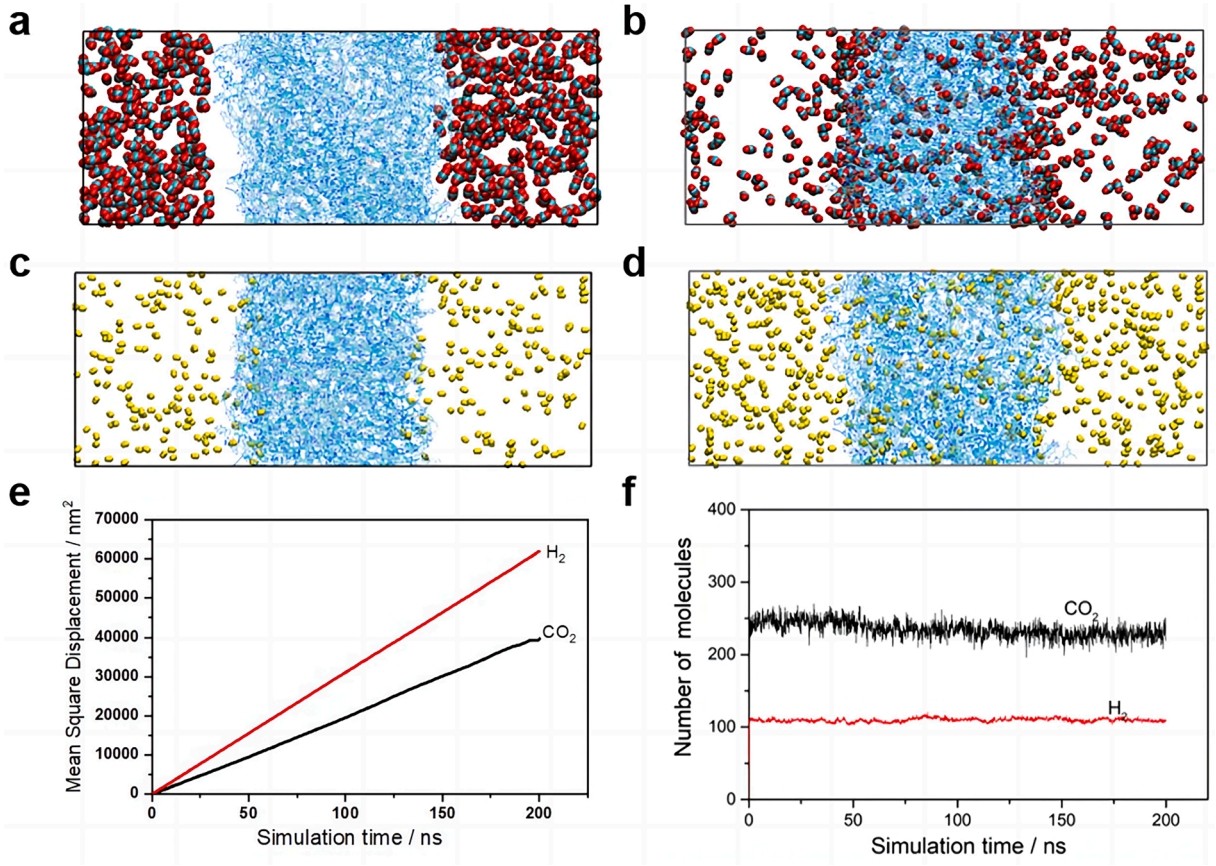

Fig. 7. Initial (a, c) and end (b, d) simulation configurations of CO_2 and H_2 diffusion in BILP-101x systems. (e) Mean square displacement (MSD) of H_2 and CO_2 along with simulation time. (f) The number of gas molecules adsorbed in the simulation system along with simulation time.

4. Conclusions

In conclusion, BILP-101x membranes with regulated micro-structure were successfully synthesized through controlling interfacial polymerization reaction time. A series of characterization techniques like PALS, PXRD, and CO_2 adsorption identified that the membranes prepared under different reaction time shows slight difference in the micro-structure and 2 h membrane has relatively high free volume and performs best for H_2/CO_2 separation. Molecular simulation demonstrates that the faster diffusion of H_2 and stronger adsorption of CO_2 in the membrane results in high H_2/CO_2 selectivity. In particular, the 2 h membrane displays an excellent H_2 permeance of 250 GPU and ultra-high H_2/CO_2 selectivity of 40 at 473 K, far surpassing the 2008 Robeson upper bound. In addition, the membrane also shows excellent H_2/N_2 and H_2/CH_4 separation performance and can withstand high temperature and pressure. The excellent separation performance, outstanding high temperature and pressure resistance together with feasible preparation, make BILP-101x membranes promising candidates for industrial application in H_2 separation and purification areas.

CRediT authorship contribution statement

Meixia Shan: Writing – original draft, Methodology, Formal analysis, Data curation. **Jingjing Zhang:** Formal analysis, Data curation. **Shenzhen Cong:** Methodology, Formal analysis, Data curation. **Yatao Zhang:** Writing – review & editing, Supervision. **Xuezhong He:** Writing – review & editing, Supervision, Funding acquisition. **Freek Kapteijn:** Writing – review & editing, Supervision, Conceptualization. **Xinlei Liu:** Writing – review & editing, Supervision, Project administration, Conceptualization.

Declaration of competing interest

The authors declare that they have no known competing financial interests or personal relationships that could have appeared to influence the work reported in this paper.

Acknowledgements

This work was supported by the National Natural Science Foundation of China (No. 52003250), the Inner Mongolia Autonomous Region Unveiling Project (No. 2022JBGS0027), the Seed Foundation of Tianjin University (No. 2023XJD-0067), the Open Project Fund from Guangdong Provincial Key Laboratory of Materials and Technology for Energy Conversion, Guangdong Technion-Israel Institute of Technology (Grant No.: MATEC2022KF005), and China Postdoctoral Science Foundation (No. 2020 M682351). The authors gratefully thank Jian Tian from Shiyanjia Lab (www.shiyanjia.com) for the model design and MD simulation.

Appendix A. Supplementary material

Supplementary data to this article can be found online at https://doi.org/10.1016/j.seppur.2024.127732.

References

[1] M. Zhang, X. Jing, S. Zhao, P. Shao, Y. Zhang, S. Yuan, Y. Li, C. Gu, X. Wang, Y. Ye, X. Feng, B. Wang, Electropolymerization of molecular-sieving polythiophene membranes for H2 separation, Angew. Chem. Int. Ed. 58 (26) (2019) 8768–8772.
[2] P.M. Falcone, M. Hiete, A. Sapio, Hydrogen economy and sustainable development goals: review and policy insights, Curr. Opin. Green. Sust. 31 (2021) 100506.

[3] T. Ashirov, A. Coskun, Ultrahigh permeance metal coated porous graphene membranes with tunable gas selectivities, Chem 7 (9) (2021) 2385–2394.
[4] L.F. Lei, F.J. Pan, A. Lindbråthen, X.P. Zhang, M. Hillestad, Y. Nie, L. Bai, X.Z. He, M.D. Guiver, Carbon hollow fiber membranes for a molecular sieve with precise-cutoff ultramicropores for superior hydrogen separation, Nat. Commun. 12 (1) (2021) 268.
[5] L. Hu, S. Pal, H. Nguyen, V. Bui, H. Lin, Molecularly engineering polymeric membranes for H_2/CO_2 separation at 100–300 °C, J. Polym. Sci. 58 (18) (2020) 2467–2481.
[6] L. Zhu, L. Huang, S.R. Venna, A.K. Blevins, Y. Ding, D.P. Hopkinson, M.T. Swihart, H. Lin, Scalable polymeric few-nanometer organosilica membranes with hydrothermal stability for selective hydrogen separation, ACS Nano 15 (7) (2021) 12119–12128.
[7] Z. Zhang, A. Simon, C. Abetz, M. Held, A.L. Höhme, E.S. Schneider, T. Segal-Peretz, V. Abetz, Hybrid organic–inorganic–organic isoporous membranes with tunable pore sizes and functionalities for molecular separation, Adv. Mater. 33 (48) (2021) 2105251.
[8] Y.B. Gu, U. Wiesner, Tailoring pore size of graded mesoporous block copolymer membranes: moving from ultrafiltration toward nanofiltration, Macromolecules 48 (17) (2015) 6153–6159.
[9] Y.Z. Zhu, L.L. Gui, R.Y. Wang, Y.F. Wang, W.X. Fang, M. Elimelech, S.H. Lin, J. Jin, Regulation of molecular transport in polymer membranes with voltage-controlled pore size at the angstrom scale, Nat. Commun. 14 (1) (2023).
[10] L. Hu, V.T. Bui, A. Krishnamurthy, S. Fan, W. Guo, S. Pal, X. Chen, G. Zhang, Y. Ding, R.P. Singh, M. Lupion, H. Lin, Tailoring sub-3.3 Å ultramicropores in advanced carbon molecular sieve membranes for blue hydrogen production, Sci 8 (2022) eabl8160.
[11] J. Wu, C.Z. Liang, A. Naderi, T.S. Chung, Tunable supramolecular cavities molecularly homogenized in polymer membranes for ultraefficient precombustion CO_2 capture, Adv. Mater. 34 (3) (2022).
[12] M. Zhao, Y.J. Ban, K. Yang, Y.W. Zhou, N. Cao, Y.C. Wang, W.S. Yang, A highly selective supramolecule array membrane made of zero-dimensional molecules for gas separation, Angew. Chem. Int. Ed. 60 (38) (2021) 20977–20983.
[13] X.C. Jing, M.X. Zhang, Z.J. Mu, P.P. Shao, Y.H. Zhu, J. Li, B. Wang, X. Feng, Gradient channel segmentation in covalent organic framework membranes with highly oriented nanochannels, J. Am. Chem. Soc. 145 (38) (2023) 21077–21085.
[14] L. Guo, Y. Shi, S. Wu, J. Jin, Z. Wang, Poly(hydrazide–imide) membranes with enhanced interchain interaction for highly selective H_2/CO_2 separation, Macromolecules 56 (9) (2023) 3430–3439.
[15] S.S. Beshahwored, M. Weber, C.-C. Hu, J.-Y. Lai, T.-S. Chung, Effects of sulfonation degree on compatibility and separation performance of polybenzimidazole (PBI)-sulfonated polyphenylenesulfone (sPPSU) blend membranes, J. Membr. Sci. 683 (2023) 121849.
[16] L. Hu, S. Fan, L. Huang, V.T. Bui, T. Tran, K. Chen, Y. Ding, M.T. Swihart, H. Lin, Supramolecular polymer networks of ion-coordinated polybenzimidazole with simultaneously improved H_2 permeability and H_2/CO_2 selectivity, Macromolecules 55 (15) (2022) 6901–6910.
[17] S. Cong, Y. Yuan, J. Wang, Z. Wang, X. Liu, Network polyimide membranes prepared by interfacial polymerization for hot H_2 purification, AICHE J 69 (4) (2022) e17983.
[18] B. Wang, Z.H. Qiao, J.Y. Xu, J.X. Wang, X.L. Liu, S. Zhao, Z. Wang, M.D. Guiver, Unobstructed ultrathin gas transport channels in composite membranes by interfacial self-assembly, Adv. Mater. 32 (22) (2020) 1907701.
[19] A. Naderi, A. Asadi Tashvigh, T.-S. Chung, H_2/CO_2 separation enhancement via chemical modification of polybenzimidazole nanostructure, J. Membr. Sci. 572 (2019) 343–349.
[20] J.H. Bitter, A., Asadi Tashvigh, Recent advances in polybenzimidazole membranes for hydrogen purification, Ind. Eng. Chem. 61 (18) (2022) 6125–6134.
[21] L.F. Villalobos, R. Hilke, F.H. Akhtar, K.V. Peinemann, Fabrication of polybenzimidazole/palladium nanoparticles hollow fiber membranes for hydrogen purification, Adv. Energy Mater. 8 (3) (2017) 1701567.
[22] L. Zhu, M.T. Swihart, H. Lin, Tightening polybenzimidazole (PBI) nanostructure via chemical cross-linking for membrane H2/CO2 separation, J. Mater. Chem. A 5 (37) (2017) 19914–19923.
[23] T.X. Yang, Y.C. Xiao, T.S. Chung, Poly-/metal-benzimidazole nano-composite membranes for hydrogen purification, Environ. Sci. Technol. 4 (10) (2011) 4171–4180.
[24] H.W.H. Lai, F.M. Benedetti, Z.X. Jin, Y.C. Teo, A.X. Wu, M.G. De Angelis, Z. P. Smith, Y. Xia, Tuning the molecular weights, chain packing, and gas-transport properties of canal ladder polymers by short alkyl substitutions, Macromolecules 52 (16) (2019) 6294–6302.
[25] M.G. Rabbani, H.M. El-Kaderi, Synthesis and characterization of porous benzimidazole-linked polymers and their performance in small gas storage and selective uptake, Chem. Mater. 24 (8) (2012) 1511–1517.
[26] T.D.M. Tessema, S.R. Venna, G. Dahe, D.P. Hopkinson, H.M. El-Kaderi, A. K. Sekizkardes, Incorporation of benzimidazole linked polymers into Matrimid to yield mixed matrix membranes with enhanced CO_2/N_2 selectivity, J. Membr. Sci. 554 (2018) 90–96.
[27] M.X. Shan, B. Seoane, A. Pustovarenko, X.R. Wang, X.L. Liu, I. Yarulina, E. Abou-Hamad, F. Kapteijn, J. Gascon, Benzimidazole linked polymers (BILPs) in mixed-matrix membranes: Influence of filler porosity on the CO_2/N_2 separation performance, J. Membr. Sci. 566 (2018) 213–222.
[28] D. Liu, C. Tian, M. Shan, J. Zhu, Y. Zhang, Interface synthesis of flexible benzimidazole-linked polymer molecular-sieving membranes with superior antimicrobial activity, J. Membr. Sci. 648 (2022) 120344.
[29] S. Duan, D. Li, X. Yang, C. Niu, S. Sun, X. He, M. Shan, Y. Zhang, Experimental and molecular simulation study of a novel benzimidazole-linked polymer membrane for efficient H_2/CO_2 separation, J. Membr. Sci. 671 (2023) 121396.
[30] A. Gao, X. Yan, S. Cong, X. Wang, H. Liu, Z. Wang, X. Liu, Designed channels in thin benzimidazole-linked polymer membranes for hot H_2 purification, J. Membr. Sci. 668 (2023) 121293.
[31] Z. Guo, S. Cong, L. Luan, M. Li, C. Luo, C. Wang, Z. Wang, X. Liu, Molecular-scale hybrid membranes: Metal-oxo cluster crosslinked benzimidazole-linked polymer membranes for superior H_2 purification, AICHE J 69 (11) (2023) e18226.
[32] X.Y. Wang, S.Z. Cong, X.R. Yan, A.T. Gao, H.F. Liu, X.L. Liu, Crosslinked benzimidazole-linked polymer membranes for dehydration of organics, Sep. Purif. Technol. 316 (2023) 123802.
[33] G.J. Zhao, L.L. Li, H.Q. Gao, Z.J. Zhao, Z.F. Pang, C.L. Pei, Z. Qu, L.L. Dong, D. W. Rao, J. Caro, H. Meng, Polyamide nanofilms through a non-isothermal-controlled interfacial polymerization, Adv. Funct. Mater. 34 (18) (2024) 2313026.
[34] X. Yan, T. Song, M. Li, Z. Wang, X. Liu, Sub-micro porous thin polymer membranes for discriminating H_2 and CO_2, Nat. Commun. 15 (1) (2024) 628.
[35] M. Shan, X. Liu, X. Wang, I. Yarulina, B. Seoane, F. Kapteijn, J. Gascon, Facile manufacture of porous organic framework membranes for precombustion CO_2 capture, Sci. Adv. 4 (9) (2018) aau1698.
[36] M.J.T. Raaijmakers, N.E. Benes, Current trends in interfacial polymerization chemistry, Prog. Polym. Sci. 63 (2016) 86–142.
[37] M. Shan, X. Liu, X. Wang, Z. Liu, H. Iziyi, S. Ganapathy, J. Gascon, F. Kapteijn, Novel high performance poly(p-phenylene benzobisimidazole) (PBDI) membranes fabricated by interfacial polymerization for H2 separation, J. Mater. Chem. A 7 (15) (2019) 8929–8937.
[38] Q.M. Gan, L.E. Peng, H. Guo, Z. Yang, C.Y. Tang, Cosolvent-assisted interfacial polymerization toward regulating the morphology and performance of polyamide reverse osmosis membranes: Increased m-phenylenediamine solubility or enhanced interfacial vaporization? Environ. Sci. Technol. 56 (14) (2022) 10308–10316.
[39] K. Li, J.Y. Zhu, D.C. Liu, Y.T. Zhang, B. Van der Bruggen, Controllable and rapid synthesis of conjugated microporous polymer membranes via interfacial polymerization for ultrafast molecular separation, Chem. Mater. 33 (17) (2021) 7047–7056.
[40] Z. Ali, F. Pacheco, E. Litwiller, Y. Wang, Y. Han, I. Pinnau, Ultra-selective defect-free interfacially polymerized molecular sieve thin-film composite membranes for H_2 purification, J. Mater. Chem. A 6 (1) (2018) 30–35.
[41] S. Karan, Z.W. Jiang, A.G. Livingston, Sub-10 nm polyamide nanofilms with ultrafast solvent transport for molecular separation, Science 348 (6241) (2015) 1347–1351.
[42] Q.Y. Zhang, X. Chen, B. Zhang, T. Zhang, W.C. Lu, Z. Chen, Z.Y. Liu, S.H. Kim, B. Donovan, R.J. Warzoha, E.D. Gomez, J. Bernholc, Q.M. Zhang, High-temperature polymers with record-high breakdown strength enabled by rationally designed chain-packing behavior in blends, Matter 4 (7) (2021) 2448–2459.
[43] J. van den Bergh, W. Zhu, J. Gascon, J.A. Moulijn, F. Kapteijn, Separation and permeation characteristics of a DD3R zeolite membrane, J. Membr. Sci. 316 (1–2) (2008) 35–45.
[44] L. Giordano, J. Gubis, G. Bierman, F. Kapteijn, Conceptual design of membrane-based pre-combustion CO_2 capture process: Role of permeance and selectivity on performance and costs, J. Membr. Sci. 575 (2019) 229–241.
[45] B. Li, Z. Wang, Z. Gao, J. Suo, M. Xue, Y. Yan, V. Valtchev, S. Qiu, Q. Fang, Self-standing covalent organic framework membranes for H_2/CO_2 separation, Adv. Funct. Mater. 33 (16) (2023) 2300219.
[46] Y.P. Ying, S.B. Peh, H. Yang, Z.Q. Yang, D. Zhao, Ultrathin covalent organic framework membranes via a multi-interfacial engineering strategy for gas separation, Adv. Mater. 34 (25) (2022) 2104946.
[47] M. Carta, R. Malpass-Evans, M. Croad, Y. Rogan, J.C. Jansen, P. Bernardo, F. Bazzarelli, N.B. McKeown, An efficient polymer molecular sieve for membrane gas separations, Science 339 (6117) (2013) 303–307.
[48] B.S. Ghanem, R. Swaidan, X. Ma, E. Litwiller, I. Pinnau, Energy-efficient hydrogen separation by ab-type ladder-polymer molecular sieves, Adv. Mater. 26 (39) (2014) 6696–6700.
[49] L.M. Robeson, The upper bound revisited, J. Membr. Sci. 320 (1–2) (2008) 390–400.
[50] B. Ashourirad, A.K. Sekizkardes, S. Altarawneh, H.M. El-Kaderi, Exceptional gas adsorption properties by nitrogen-doped porous carbons derived from benzimidazole-linked polymers, Chem. Mater. 27 (4) (2015) 1349–1358.